Shell Model for Buoyancy-Driven Turbulent Flows

Abhishek Kumar* and Mahendra K. Verma+

Department of Physics, Indian Institute of Technology Kanpur, Kanpur, 208016, India

**E-mail: abhkr@iitk.ac.in* +*E-mail: mkv@iitk.ac.in*

In this paper we construct a comprehensive shell model for the buoyancy-driven turbulence, which is applicable to convective turbulence and stably-stratified turbulence. We simulate these models in the turbulent regime and show that the stably-stratified turbulence exhibit Bolgiano-Obukhbov scaling ($E(k) \sim k^{-11/5}$), and the convective turbulence shows Kolmogorov spectrum ($E(k) \sim k^{-5/3}$).

Keywords: Shell model; Buoyancy-driven turbulence; Rayleigh Bénard convection.

1. Introduction

Turbulent fluid flows exhibit complex behaviour. Strong nonlinear interactions among large number of modes of a turbulent flow makes the theoretical analysis highly intractable. Shell models are simplified sets of the equations of fluid mechanics in wavenumber space. They are low-dimensional models which are successful in explaining some features of turbulence[1,2], e.g., the models for fluid turbulence reproduce the Kolmogorov's theoretical predictions. In a shell model, the wavenumber space is logarithmically divided into N shells, where N is the total number of shells. The energy exchange takes place between three nearest neighbouring shells, e.g. $(n+1, n, n-1)$, and each shell contains only one mode. A major advantage of shell model over direct numerical simulation (DNS) is its ability to solve flow simulations with very high Reynolds number (Re). For instance, a DNS of a turbulent flow with $\mathrm{Re} \approx 10^9$ would require $\mathrm{Re}^{9/4} \approx 10^{81/4} \approx 2 \times 10^{20}$ grid points and significantly large computational time, which are impossible even in most sophisticated supercomputers of today, but such large-Re flows can be approximately solved using a shell model with $N = 76$. We remark that in the present paper we have performed shell model simulation for $\mathrm{Re} \approx 10^9$ (see Table I). A point to note is that the shell model assume

spherical isotropy in wavenumber space.

There have been several advances in understanding of fluid turbulence using shell model. However, till date, no convergence has been reached on the shell model for buoyancy driven turbulence[3–5], which is very important in the flows of geophysics, astrophysics, atmospheric and solar physics, as well as in engineering. Buoyancy-driven flows exhibit variety of phenomena—waves, patterns, weak turbulence, and strong turbulence (see the companion paper by Verma *et al.*[6] in this volume). Turbulence in buoyancy-induced flows come in two categories: (a) convective turbulence in which the hotter and lighter fluid at the bottom rises, while the colder and heavier fluid at the top comes down. These flows are unstable; (b) Stably-stratified turbulence in which the lighter fluid is above the heavier fluid.

The shell models describe the turbulent flows in the isotropic regime, hence we limit ourselves to the isotropic turbulent flows. For the isotropic stably-stratified flows, the buoyancy should be smaller than the nonlinear term $\mathbf{u} \cdot \nabla \mathbf{u}$ that corresponds to Richardson number (the ratio of buoyancy and nonlinear term) less than unity. Strong buoyancy leads to quasi two-dimensionality[7,8], whose analysis is beyond the scope of the shell model. For the convective turbulence, the flow is approximately isotropic[9,10], hence it can be analysed using a shell model.

For stably stratified flows, Bolgiano[11] and Obukhov[12] first proposed a phenomenology, according to which the kinetic energy (KE) spectrum $E_u(k) \sim k^{-11/5}$, the entropy spectrum $E_\theta(k) \sim k^{-7/5}$, KE energy flux $\Pi_u(k) \sim k^{-4/5}$, and entropy flux $\Pi_\theta(k) =$ constant. This scaling is referred to as Bolgiano-Obukhov (BO) phenomenology[6,13,14]. Here $\mathbf{u}$ and θ are the velocity and temperature fluctuations.

Since buoyancy drives the convective turbulence, Procaccia and Zeitak[15], and L'vov[16] proposed the BO scaling for convective turbulence as well. However Kumar *et al.*[13] showed that the energy flux for the convective turbulence does not decrease with wavenumber since buoyancy feeds the kinetic energy (contrary to BO scaling). Kumar *et al.*[13] analyzed the energy spectrum and the energy feed due to buoyancy for the Rayleigh Bénard convection, and showed that for a set of parameters, the kinetic energy feed due to the buoyancy was compensated by the dissipation rate in a region of wavenumbers, for which they observed Kolmogorov's spectrum.

In the present paper we provide a comprehensive shell model for the buoyancy-induced turbulence, and show that the kinetic energy spectrum in Rayleigh Bénard convection is close to Kolmogorov's theory of fluid tur-

bulence, while that in stably-stratified flows is proportional to $k^{-11/5}$. We also show the existence of ultimate regime[17] in shell model for convective turbulence. For convective turbulence, we have computed the Richardson number and compare it with the Péclet number scaling, similar to the analysis for Verma *et al.*[6]. Our shell model results are consistent with the numerical findings of Kumar *et al.*'s[13].

2. Shell Model for Buoyancy-Induced Turbulence

A Sabra shell model[18,19] of buoyancy-driven turbulence under Boussinesq approximations is

$$\frac{du_n}{dt} = N_n[u,u] + \alpha g\theta_n - \nu k_n^2 u_n + f_n, \tag{1}$$

$$\frac{d\theta_n}{dt} = N_n[u,\theta] - \frac{d\bar{T}}{dz}u_n - \kappa k_n^2\theta_n, \tag{2}$$

where u_n is the velocity shell variable, θ_n is the shell variable for the temperature fluctuations, f_n is the external forcing, g is acceleration due to gravity, α, ν, κ are the thermal expansion coefficient, the kinematic viscosity, and the thermal diffusivity respectively, and $k_n = k_0\lambda^n$ is the wavenumber of the shell. Since the shell models are applicable to a periodic box without walls, the above can be considered as a part of an unbound system with a vertical temperature gradient of $d\bar{T}/dz$.

In convective turbulence, the buoyancy compensates the dissipative losses, hence the shell model for convection does not require any external forcing to maintain a steady state. However, the shell model for the stably stratified turbulence needs to be forced for obtaining a steady state. In our shell-model simulations of stably stratified turbulence, we force n_f small wavenumber shells randomly so as to feed a constant energy supply rate ε to the system. The energy supply rate ε is divided equally to the n_f shells, hence

$$f_n = \sqrt{\frac{\varepsilon}{n_f \Delta t}}\exp(i\phi_n) \tag{3}$$

where ϕ_n is the random phase of the nth shell chosen from the uniform distribution in $[0, 2\pi]$. In our simulation we force the shells $n = 3$ and 4, hence $n_f = 2$.

The nonlinear terms $N_n[u,u]$ and $N_n[u,\theta]$ of the above equations are

$$N_n[u,u] = -i(a_1 k_n u_{n+1}^* u_{n+2} + a_2 k_{n-1} u_{n-1}^* u_{n+1} - a_3 k_{n-2} u_{n-1} u_{n-2}) \tag{4}$$

$$\begin{aligned} N_n[u,\theta] = -i[&k_n(d_1 u_{n+1}^*\theta_{n+2} + d_3\theta_{n+1}^* u_{n+2}) \\ &+k_{n-1}(d_2 u_{n-1}^*\theta_{n+1} - d_3\theta_{n-1}^* u_{n+1}) \\ &-k_{n-2}(-d_1 u_{n-1}\theta_{n-2} - d_2\theta_{n-1}u_{n-2})] \end{aligned} \tag{5}$$

where $a_1 = d_1 = 1$, $a_2 = d_2 = \lambda - 2$, and $a_3 = d_3 = 1 - \lambda$, where λ is chosen as golden mean whose value is $(\sqrt{5}+1)/2$[1]. The above model conserves kinetic energy $\sum_n u_n^2/2$ when the viscous and the buoyancy terms are turned off. $N[u,\theta]$ is chosen as above so that

$$\Re\left(\sum_n \theta_n^* N_n[u,\theta]\right) = 0, \tag{6}$$

where $\Re$ is the real part of the argument.

It is convenient to work with the nondimensionalized equations, which is achieved by using the characteristic length d as the length scale, $\sqrt{\alpha g|d\bar{T}/dz|d^2}$ as the velocity scale, and $|d\bar{T}/dz|d$ as the temperature scale. Therefore, $u_n = u_n'\sqrt{\alpha g|d\bar{T}/dz|d^2}$, $\theta_n = \theta_n'|d\bar{T}/dz|d$, $k_n = k_n'/d$, and $t = t'(d/\sqrt{\alpha g|d\bar{T}/dz|d^2})$. In terms of nondimensonalized variables, the equations are

$$\frac{du_n'}{dt'} = N_n'[u',u'] + \theta_n' - \sqrt{\frac{\mathrm{Pr}}{\mathrm{Ra}}}k_n'^2 u_n' + f_n', \tag{7}$$

$$\frac{d\theta_n'}{dt'} = N_n'[u',\theta'] - Su_n' - \frac{1}{\sqrt{\mathrm{RaPr}}}k_n'^2\theta_n', \tag{8}$$

where $S = (d\bar{T}/dz)/(\Delta/d)$, where Δ is the absolute temperature differences in height d. $S = 1$ for positive $d\bar{T}/dz$ (stably stratified flows), and $S = -1$ for negative $d\bar{T}/dz$ (convective flows).

The two nondimensional control parameter in the above equations are Rayleigh number Ra, which is a ratio of the buoyancy force and dissipative force, and the Prandtl number Pr, which is a ratio of the kinematic viscosity and the thermal diffusivity. We also remark that our shell model differs from that of Brandenburg[3].

A stably-stratified flows are stable, hence the fluctuations would vanish asymptotically. Hence, to generate turbulence in stably-stratified flow, we force the large scale flows. We apply forcing f_n to shells with small n that represents large length scales. Note that for $f_n = 0$, we obtain $u_n \to 0$ and $\theta_n \to 0$ asymptotically.

3. Numerical Methods

We simulate the shell models by solving Eqs. (7) and (8). For stably-stratified turbulence, $S = 1$, but for convective turbulence, $S = -1$. For time stepping we use fourth-order Runge-Kutta (RK4) method. We took 76 shells for the convective turbulence simulations, and 36 shells for the stratified turbulence simulations. For both convective and stably stratified turbulence we take $\mathrm{Pr} = 1$.

For the stably-stratified turbulence, we performed two sets of simulations, one with $\mathrm{Ra} = 10^5$ and the other with $\mathrm{Ra} = 10^{10}$. To generate turbulence, we employ random forcing to the shells 2 to 4. The Richardson number, which is a ratio of the buoyancy term and the nonlinear term $\mathbf{u} \cdot \nabla \mathbf{u}$, is an important parameter for stably stratified turbulence. We compute the spectra and fluxes of the kinetic energy and entropy $(\theta^2/2)$ by averaging over many time frames ($\sim 10^8$) of the steady-state flow.

Table I. Parameters of our simulations of convective turbulence: Rayleigh number Ra, Nusselt number Nu, Reynolds number Re, kinetic energy dissipation rate ϵ_u, entropy dissipation rate ϵ_θ, and Kolmogorov's constant K_{Ko}. We choose number of shells $N = 76$ and Prandtl number $\mathrm{Pr} = 1$ for all our runs.

Ra	Nu	Re	ϵ_u	ϵ_θ	K_{Ko}
10^{10}	6.0×10^6	8.6×10^5	36.5	48.8	1.2
10^{11}	1.9×10^7	2.7×10^6	76.5	61.8	0.9
10^{12}	6.4×10^7	8.7×10^6	51.0	54.3	1.0
10^{13}	1.9×10^8	2.7×10^7	61.8	80.6	0.9
10^{14}	6.4×10^8	8.7×10^7	36.4	48.5	1.2
10^{15}	2.2×10^9	2.9×10^8	94.1	95.2	0.9
10^{16}	6.7×10^9	8.9×10^8	42.1	108.1	1.1

For convective turbulence, we perform simulations for various Rayleigh numbers as listed in Table I and compute various quantities listed in Table I

using the steady-state data. We also compute the Nusselt number for different Ra's and derive a scaling relationship between Nu with Ra. Note that the Nusselt number is the ratio of the total (convective plus conductive) heat flux to the conducive heat flux, and it is expressed as[20]

$$\mathrm{Nu} = \frac{-\kappa \frac{d\bar{T}}{dz} + \langle u_n \theta_n \rangle}{-\kappa \frac{d\bar{T}}{dz}} = 1 - \left\langle \frac{u_n}{\kappa} \frac{\theta_n}{\frac{d\bar{T}}{dz}} \right\rangle = 1 + \sqrt{\mathrm{RaPr}} \langle u'_n \theta'_n \rangle. \quad (9)$$

Here the nondimensionalized shell velocity and temperature field are $u'_n = u_n / \sqrt{\alpha g d^2 d\bar{T}/dz}$ and $\theta' = (\theta/d)/(d\bar{T}/dz)$ respectively.

4. Results and Discussions

4.1. *Shell model for stably-stratified turbulence*

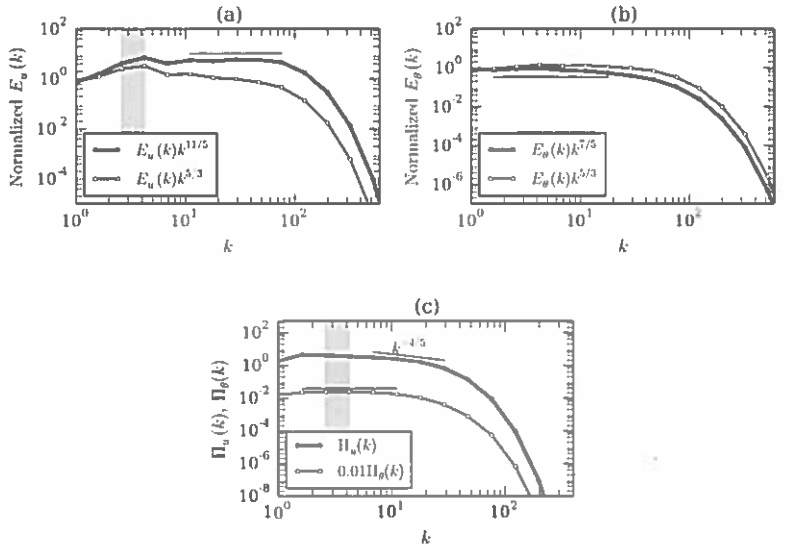

Fig. 1. Stably stratified turbulence with $\mathrm{Pr} = 1$, $\mathrm{Ra} = 10^5$, and $\mathrm{Ri} = 0.10$: plots of (a) normalized KE spectra, (b) normalized entropy spectra and (c) KE flux $\Pi_u(k)$ and entropy flux $\Pi_\theta(k)$. The plots shows that *BO* scaling fits with the data better than the *KO* scaling.

For stably stratified flow, we take $\mathrm{Pr} = 1$, $\mathrm{Ra} = 10^5$. The energy supply rate was chosen to be $\varepsilon = 50$. Under steady state, we achieved $\mathrm{Ri} = 0.10$, Reynolds number $\mathrm{Re} = 10^3$, kinetic energy dissipation rate $\epsilon_u = 3.9$, and entropy dissipation rate $\epsilon_\theta = 3.1$. In Fig. 1(a) we plot the normalized KE

spectra, $E_u(k)k^{11/5}$ for the *BO* scaling, and $E_u(k)k^{5/3}$ for the *KO* scaling. Shadow region in the figure is the forcing band. In Fig. 1(b) we plot the normalized entropy spectra, $E_\theta(k)k^{7/5}$ for the *BO* scaling, and $E_\theta(k)k^{5/3}$ for the *KO* scaling. The figure indicates that the *BO* scaling fits with the numerical data better than *KO* scaling. Along with the spectrum results, we also compute the KE and entropy fluxes, which are plotted in Fig. 1(c). $\Pi_u(k) \sim k^{-4/5}$, and Π_θ = const (though not in the same wavenumber range), consistent with *BO* scaling. These results show that *BO* scaling is valid for stably stratified flow. We find that the energy supply rate by buoyancy, $F(k) = \Re\langle u_k \theta_k^* \rangle$, is negative, indicating a conversion of kinetic energy to the potential energy[13]. We obtain an approximate dual scaling

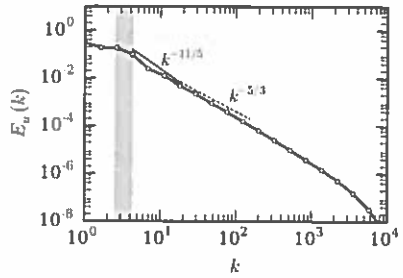

Fig. 2. Stably stratified turbulence with Pr = 1, Ra = 10^{10} and Ri = 0.25: plot of KE spectrum. The wavenumber range $4 < k < 18$ exhibit $E(k) \sim k^{-11/5}$, and $18 < k < 100$ exhibit $E(k) \sim k^{-5/3}$.

($k^{-11/5}$ and $k^{-5/3}$) for Ra = 10^{10}. For this run we keep $\varepsilon = 10$, and under steady state we achieved Ri = 0.25, Re = 2×10^5, $\epsilon_u = 0.6$, and $\epsilon_\theta = 0.8$. It turns out that the dual scaling occurs for a very narrow set of parameters for which the buoyancy is strong, but not so strong so as to make the flow quasi two-dimensional.

In addition, for small Richardson number or for weak buoyancy, we obtain Kolmogorov's $k^{-5/3}$ energy spectrum. The aforementioned results are consistent with the DNS results of Kumar *et al.*[13].

4.2. *Convective turbulence shell model*

The parameters used for the convective turbulence simulations are listed in Table I. For one of the runs, Ra = 10^{16} and Pr = 1, we plot the normalized KE spectrum, $E_u(k)k^{5/3}$, and the normalized entropy spectrum, $E_\theta(k)k^{5/3}$ in Fig. 3(a). The figure indicates that Kolmogorov (*KO*) scaling fits quite

well with the data for three decades. We cross check our spectrum result with the KE and entropy fluxes, which are plotted in Figs. 3(b) and 3(c) respectively. The KE flux $\Pi_u(k)$ slightly increases with k (see Fig. 3(b)) as shown by dashed red curve and then becomes constant. The entropy flux $\Pi_\theta(k)$ remains constant in the inertial range. These results demonstrate that the Kolmogorov scaling is valid for the convective turbulence.

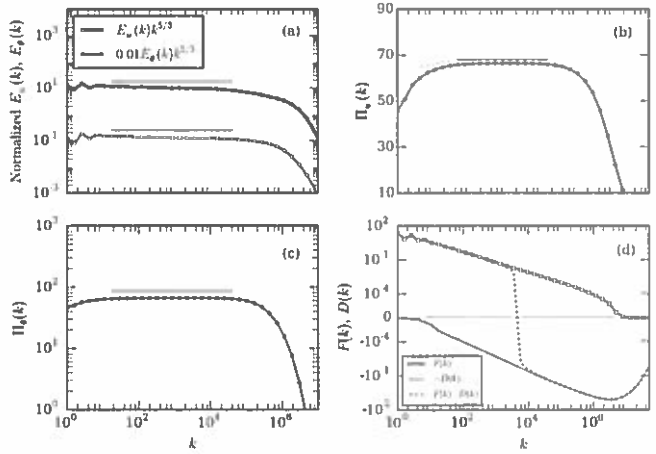

Fig. 3. Convective turbulence with Pr = 1 and Ra = 10^{16}: plots of (a) normalized KE spectra and normalized entropy spectra for Kolmogorov-Obukhov (*KO*) scaling, (b) KE flux $\Pi_u(k)$ and (c) entropy flux $\Pi_\theta(k)$, and (d) energy supply rate $F(k)$, dissipation rate $D(k)$, and $F(k) - D(k)$.

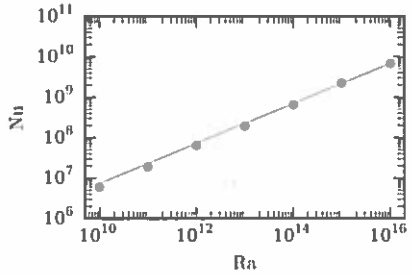

Fig. 4. Plot of the Nusselt number Nu versus Ra. The function Nu = $(86.4 \pm 18.7)\mathrm{Ra}^{(0.49 \pm 0.01)}$ fits well with the simulation data.

We also compute energy supply rate $F(k) = \Re\langle u_k \theta_k^* \rangle$ and plot it in Fig. 3(d). The plot indicates a positive energy transfer from buoyancy to the kinetic energy[13]. In Fig. 3(d), we also plot the dissipation rate $D(k)$

and $F(k) - D(k)$. $F(k)$ and $D(k)$ cancel each other in the inertial range, and hence $d\Pi_u(k)/dk \approx 0$ or $\Pi(k)$ is approximately constant. This yields a constant KE flux $\Pi_u(k)$ which leads to Kolmogorov's spectrum.

We compute the Richardson number for all convection runs, and observe it to be approximately 0.01. The above number is related to the Péclet number:

$$\begin{aligned} \mathrm{Ri} &= \frac{\alpha g d(d\bar{T}/dz)}{u^2/d} \\ &= \frac{\alpha g d^1(d\bar{T}/dz)}{\nu\kappa}\frac{\nu}{\kappa}\frac{\kappa^2}{u^2 d^2} \\ &= \frac{\mathrm{RaPr}}{\mathrm{Pe}^2} \end{aligned} \tag{10}$$

where Pe is the Péclet number. Verma *et al.*[20] showed that

$$\mathrm{Pe} = C\sqrt{\mathrm{RaPr}}. \tag{11}$$

In our numerical simulations of shell model for the convective turbulence, we observe that $C \approx 10$, hence $\mathrm{Ri} \approx 0.01$. Since Richardson number is relatively small, the nonlinear term dominates the buoyancy term; the observed Kolmogorov's spectrum is possibly because of this reason.

Since the Prandtl number is unity, the Reynolds number ud/ν is same as the Péclet number, and it is listed in Table I for all the runs. We compute the Kolmogorov constant K_{Ko} using the energy spectrum and the energy flux. We observe that K_{Ko} listed in Table I ranges from 0.9 to 1.2. We compute the Nusselt number using Eq. (9), and plot it in Fig. 4 as a function of Ra. The best fit of our data is $\mathrm{Nu} = (86.4 \pm 18.7)\mathrm{Ra}^{(0.49\pm0.01)}$. This result is consistent with Kraichnan's predication[17], according to which $\mathrm{Nu} \sim \mathrm{Ra}^{1/2}$ for very high Rayleigh numbers (called the ultimate regime).

5. Summary and Conclusions

In summary, we constructed a combined shell models for convective turbulence and stably-stratified turbulence. The difference in these models is in the temperature gradient term of the temperature equation. Using numerical computation of these models we demonstrate the stably-stratified turbulence shows Bolgiano-Obukhov scaling, while the convective turbulence exhibits Kolmogorov spectrum. These results are consistent with the recent numerical results of Kumar *et al.*[13,14] which are based on pseudospectral simulation. We remark that the Bolgiano-Obukhov scaling for stably stratified flow is observed for the isotropic turbulence which is observed when the Froude number is of the order of unity.

6. Acknowledgments

We thank K. R. Sreenivasan for useful comments during the IUTAM meeting, and T. K. Sengupta and the organizers for hosting the wonderful and interactive IUTAM meeting. We also thanks the editors of the proceedings for the useful suggestions on the paper. This work was supported by a research grant SERB/F/3279/2013-14 from Science and Engineering Research Board, India.

References

1. P. Ditlevsen, *Turbulence and Shell Models* Cambridge Univ. Press, Cambridge, UK (2011).
2. L. Biferale, *Ann. Rev. Fluid Mech.* **35**, 441 (2003).
3. A. Brandenburg, *Phys. Rev. Lett.* **69**, 605 (1992).
4. J. Mingshun and L. Shida, *Phys. Rev. E* **56**, 441 (1997).
5. E. S. C. Ching and W. C. Cheng, *Phys. Rev. E.* **77**, 015303 (2008).
6. M. K. Verma, A. Kumar, and A. G. Chatterjee, Under review in IUTAM proceedings (2015).
7. E. Lindborg, *Geo. Res. Lett.* **32**, L01809 (2005).
8. E. Lindborg, *J. Fluid Mech.* **550**, 207 (2006).
9. B. Dutta and M. K. Verma, Unpublished (2015).
10. A. Pandey, M. K. Verma, and P. K. Mishra *Phys. Rev. E* **89**, 023006 (2014).
11. R. Bolgiano, *J. Geophys. Res.* **64**, 2226 (1959).
12. A. N. Obukhov, *Dokl. Akad. Nauk SSSR* **125**, 1246 (1959).
13. A. Kumar, A. G. Chatterjee, and M. K. Verma, *Phys. Rev. E* **90**, 023016 (2014).
14. M. K. Verma, A. Kumar, and A. G. Chatterjee, *Phys. Focus* **25**(1), 45 (2015).
15. I. Procaccia and R. Zeitak, *Phys. Rev. Lett.* **62**, 2128 (1989).
16. V. S. L'vov, *Phys. Rev. Lett.* **67**, 687 (1991).
17. R. H. Kraichnan, *Phys. Fluids* **5**, 1374 (1962).
18. V. L'vov, E. Podivilov, A. Pomyalov, I. Procaccia, and D. Vandembroucq, *Phys. Rev. E* **58**, 1811 (1998).
19. A. Kumar and M. K. Verma, *Phys. Rev. E* **91**, 043014 (2015).
20. M. K. Verma, P. K. Mishra, A. Pandey, and S. Paul, *Phys. Rev. E* **85**, 016310 (2012).